Journal of the Physical Society of Japan
Vol. 75, No. 5, May, 2006, 051012


SPECIAL TOPICS

*Organic Conductors*

# *d*-wave Pair Symmetry in the Superconductivity of $\kappa$-(BEDT-TTF)$_2$X

Koichi ICHIMURA* and Kazushige NOMURA†

*Division of Physics, Hokkaido University, Sapporo 060-0810*

(Received December 6, 2005; accepted December 21, 2005; published May 10, 2006)

The superconducting phase of organic superconductors $\kappa$-(BEDT-TTF)$_2$X was studied by the electron tunneling using scanning tunneling microscope (STM). Tunneling both at the conducting plane and lateral surfaces was performed on single crystals of $\kappa$-(BEDT-TTF)$_2$Cu(NCS)$_2$. Tunneling conductance curve obtained at the conducting plane is explained by the *d*-wave gap symmetry. The temperature dependence of tunneling spectra is also consistent with the *d*-wave symmetry. Tunneling spectra at lateral surfaces varies depending on the tunneling direction, suggesting the in-plane anisotropy of the gap. The directional dependence is also consistent with the *d*-wave symmetry with line nodes $\pi/4$ from the $k_b$- and $k_c$-axes. It indicates that the superconducting pair wave function has the $d_{x^2-y^2}$-wave symmetry. (If we take the same conventions for the magnetic Brillouin zone as high-$T_c$ cuprates with the $d_{x^2-y^2}$-wave symmetry, the gap symmetry of $\kappa$-(BEDT-TTF)$_2$Cu(NCS)$_2$ is the $d_{xy}$-wave symmetry.) Protonated and partially deuterated $\kappa$-(BEDT-TTF)$_2$Cu[N(CN)$_2$]Br were also studied. Tunneling spectra are consistent with the *d*-wave symmetry in all salts. Gap parameters obtained in each salt were discussed in the view point of the effective correlation. The large gap value suggests the strong coupling superconductivity. The pseudogap structure was found above $T_c$. The zero bias conductance peak, which gives an evidence for nodes of the superconducting gap, was found.

KEYWORDS: organic superconductor, scanning tunneling spectroscopy, pairing symmetry, $\kappa$-(BEDT-TTF)$_2$X
DOI: 10.1143/JPSJ.75.051012

## 1. Introduction

Organic superconductors $\kappa$-(BEDT-TTF)$_2$X[1)] are characterized by their layered structure. Conducting BEDT-TTF layers are separated by insulating anion layers. The electronic band has rather two dimensional character. The band filling is half-filled due to the dimerization of BEDT-TTF molecules. The on-site Coulomb interaction between electrons is comparable to the band width in this system. Therefore, $\kappa$-(BEDT-TTF)$_2$X family exhibits the Mott transition. The quasi-two dimensional electronic band with the strong electron correlation plays an important role in the electronic behaviors of $\kappa$-(BEDT-TTF)$_2$X, similarly to the high-$T_c$ superconducting oxides. It is recognized that the superconducting phase adjoins the antiferromagnetic phase[2)] in contrast to the high-$T_c$ cuprates in which these phases are separated by the anomalous metallic phase.[3)] A lot of attentions have been attracted to which mechanism brings about the superconductivity in the neighborhood of the Mott insulating phase. In these highly correlated system, the unconventional mechanism of the superconductivity is suggested. The *d*-wave pairing has been discussed from several origins theoretically.[4–6)] Various kinds of experiments have so far been performed to investigate the pairing symmetry. From the temperature dependence of the Knight shift $K_s(T)$ below the superconducting transition temperature $T_c$,[7,8)] it is recognized that the electron pair is in the spin-singlet state. This means that the *s*- and *d*-wave symmetry are suitable candidates for the superconducting gap symmetry. The $^{13}$C nuclear magnetic resonance (NMR) spin–lattice relaxation rate $T_1^{-1}(T)$ follows a $T^3$ low at low temperature.[7–9)] The electronic specific heat $C_{el}(T)$ exhibits $T^2$-dependence below 1 K.[10)] Several results of the magnetic field penetration depth $\lambda(T)$ follow a power low.[11–15)] These are consistent with the the line nodes structure in the *d*-wave symmetry. On the other hand, in some other experiments of $\lambda(T)$[16–18)] and $C_{el}(T)$[19)] the temperature dependence follows the thermal activating exponential law, which supports the full-gap *s*-wave symmetry. Recently, Izawa *et al.*[20)] measured the thermal conductivity in the mixed state of $\kappa$-(BEDT-TTF)$_2$Cu(NCS)$_2$ with rotating the magnetic field in the conducting plane and discussed the gap anisotropy. The angular dependence of the electronic thermal conductivity has a fourfold symmetry, which is consistent with the *d*-wave paring.

For the investigation of the electronic state in the superconducting phase, the electron tunneling is very powerful because the electronic density of states can be obtained directly with the high energy resolution.[21)] The tunneling spectroscopy using the scanning tunneling microscope (STM), i.e., the scanning tunneling spectroscopy (STS), especially has a great advantage because of non-contacting tip configuration. The usefulness of the STS has been demonstrated with the observation of the local electronic density of states in the superconducting phase. The energy-resolved microscopic structure of the magnetic fluxoid in 2*H*-NbSe$_2$[22)] and the quasi-particle scattering resonance at impurity sites in Bi$_2$Sr$_2$CaCu$_2$O$_8$[23)] were observed clearly with atomic resolution with use of the STS. For $\kappa$-(BEDT-TTF)$_2$Cu(NCS)$_2$, we have reported that the superconducting gap is highly anisotropic.[24,25)] The result is consistent with the first STS work by Bando *et al.*[26)]

The bound state arising on the gap node is an important feature which characterizes anisotropic superconductors with line nodes, since it reflects the phase interference of the order parameter. Such a bound state is observed as the zero bias conductance peak (ZBCP) in tunneling spectra.[28)]

*E-mail: ichimura@sci.hokudai.ac.jp
†E-mail: knmr@phys.sci.hokudai.ac.jp

The ZBCP is observed popularly in high-$T_c$ cuprates[29–31] whose pairing symmetry is of the $d$-wave. Although the $d$-wave pairing has been suggested in $\kappa$-(BEDT-TTF)$_2$X, the ZBCP has not been observed yet.

The phase diagram of $\kappa$-(BEDT-TTF)$_2$X with respect to the effective correlation strength, which is controlled by the effective pressure, i.e., the physical or chemical one (substitution of anion molecules and modification of donor molecules), has been proposed.[2] In the phase diagram, the superconducting phase appears in the neighborhood of the insulating antiferromagnetic phase, which is recognized as the Mott insulating state. The superconducting transition temperature $T_c$ increases with increasing the effective correlation toward the phase boundary. As we describe below, we are interested in $\kappa$ type BEDT-TTF salts of $\kappa$-(BEDT-TTF)$_2$Cu(NCS)$_2$ ($T_c \simeq 10$ K) and $\kappa$-(BEDT-TTF)$_2$-Cu[N(CN)$_2$]Br ($T_c \simeq 11.5$ K). The salt of $\kappa$-(BEDT-TTF)$_2$-Cu[N(CN)$_2$]Br, which has higher effective correlation than $\kappa$-(BEDT-TTF)$_2$Cu(NCS)$_2$, is located near the boundary between the superconducting and antiferromagnetic phases. The deuteration of end protons of the BEDT-TTF molecule is useful method to tune finely the band width and correlation strength. Protonated d[0,0] salt undergoes the superconducting transition while fully deuterated d[4,4] salt is just on the phase boundary. Kawamoto *et al.*[27] demonstrated that the effective correlation can be controlled finely near the Mott boundary by partial deuteration of BEDT-TTF molecules.

In this article, we describe the electron tunneling measurements using STM in $\kappa$-(BEDT-TTF)$_2$X and discuss the $d$-wave pairing symmetry. In §3.1, we present the STS results on the conducting plane of $\kappa$-(BEDT-TTF)$_2$-Cu(NCS)$_2$ and discuss the functional form of tunneling spectra. We also discuss the temperature dependence of the tunneling conductance curve at low temperature. Direct observation of the $d$-wave anisotropy of the superconducting gap is given by the tunneling at the lateral surfaces of $\kappa$-(BEDT-TTF)$_2$Cu(NCS)$_2$ in §3.2. The gap parameter in partially deuterated $\kappa$-(BEDT-TTF)$_2$Cu[N(CN)$_2$]Br is discussed with respect to the effective correlation strength in §3.3. The pseudogap in $\kappa$-(BEDT-TTF)$_2$X is discussed in §3.4. We also present the first observation of the ZBCP in organic superconductors in §3.5.

## 2. Experimental

Single crystals of $\kappa$-(BEDT-TTF)$_2$X were grown by the electro-crystallization method.[32] The typical size of a single crystal used in the present STS experiment was $1 \times 1 \times 0.1\,\mathrm{mm}^3$. A gold wire of 50 µm in diameter was attached to the crystal with gold paste as a current lead. We investigated both the $b$–$c$ and lateral surfaces for $\kappa$-(BEDT-TTF)$_2$-Cu(NCS)$_2$, and the $a$–$c$ surface for protonated and partially deuterated $\kappa$-(BEDT-TTF-d[$n$,$n$])$_2$Cu[N(CN)$_2$]Br. As-grown surfaces were investigated directly without any special surface treatment. Samples of $\kappa$-(BEDT-TTF-d[$n$,$n$])$_2$-Cu[N(CN)$_2$]Br were cooled slowly around 80 K with the cooling rate of less than 0.1 K/min, because the low temperature electronic state depends on the cooling rate. The sample was mounted in the STM unit installed in the thermal cell filled with low-pressure helium exchange gas, and cooled down to 1.2 K. A mechanically sharpened Pt–Ir alloy wire attached to the top of the tube piezoelectric scanner was used as the STM tip. The differential tunneling conductance $\mathrm{d}I/\mathrm{d}V$ was directly measured by the lock-in detection, in which 1 kHz AC modulation with amplitude of 0.1 mV was superposed in the ramped bias voltage. The STM apparatus was mounted on the vibrational isolator with the air suspension. The vibrational isolator stands on the floor, which is vibrationally isolated from the building floor.

## 3. Results and Discussion

### *3.1 Tunneling spectra on the b–c surface of κ-(BEDT-TTF)$_2$Cu(NCS)$_2$*

At first, we investigated the tunneling differential conductance at the conducting $b$–$c$ surface of $\kappa$-(BEDT-TTF)$_2$Cu(NCS)$_2$. In this configuration, the tunneling current flows perpendicular to the conducting plane. Figure 1 shows a typical tunneling conductance curve. The superconducting gap structure is clearly recognized in tunneling spectra. The conductance at zero bias voltage is well reduced. The gap edge is observed as shoulders around $|V| = 2.5$ mV. Inside the gap edge, the conductance depends linearly on the energy in contrast to the case of the $s$-wave symmetry, suggesting the gap anisotropy. We examine the obtained curve with the simple $d$-wave gap model described as $\Delta(\boldsymbol{k}) = \Delta_0 \cos 2\theta$. Here $\Delta_0$ and $\theta$ are the maximum value of the gap and the azimuthal angle in $\boldsymbol{k}$-space, respectively. In this tunneling configuration, each direction component in $\boldsymbol{k}$-space contributes equally to the tunneling current. As a result, the total tunneling conductance curve is given as

$$\frac{\mathrm{d}I}{\mathrm{d}V} \propto \int_0^{2\pi}\int_{-\infty}^{\infty} \mathrm{Re}\left[\frac{|E - \mathrm{i}\Gamma|}{\sqrt{(E-\mathrm{i}\Gamma)^2 - \Delta^2(\theta)}}\right] \times \left\{-\frac{\partial f(E+eV)}{\partial V}\right\} \mathrm{d}E\,\mathrm{d}\theta, \tag{1}$$

where $\Gamma$ is the broadening parameter of the one-electron level[33] and $f(E)$ is the Fermi–Dirac distribution function. The broken line in Fig. 1 represents the fitting by the model with $\Delta_0 = 3.0$ meV and $\Gamma = 0.10$ meV. The value of $\Gamma$ is

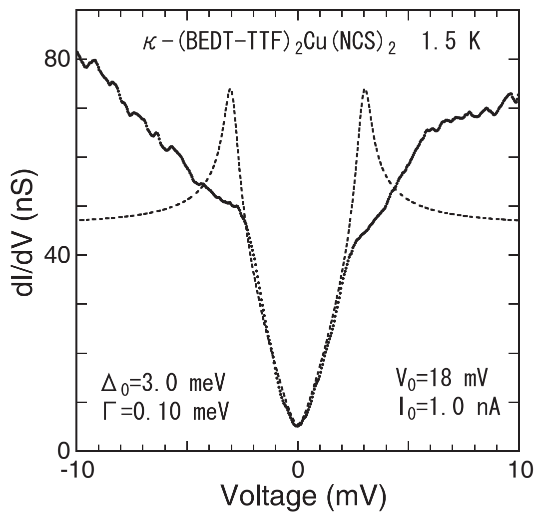


Fig. 1. Typical tunneling conductance curve obtained at the $b$–$c$ surface of $\kappa$-(BEDT-TTF)$_2$Cu(NCS)$_2$ at 1.5 K. The broken line represents the calculated curve for the $d$-wave gap model with $\Delta_0 = 3.0$ meV and $\Gamma = 0.10$ meV.

sufficiently small as compared with $\Delta_0$. It assures the validity of the argument about the pairing symmetry in our tunneling spectra. As shown in the figure, conductance curve in low-energy region, in which the symmetry of the gap is essentially reflected, is well fitted by the model. The gap structure observed in the *b*–*c* plane is consistent with the *d*-wave pairing symmetry.

The gap parameter varies slightly from sample to sample. We obtain the gap value as $\Delta_0 = 2.5-4.9$, correspondingly $2\Delta_0/kT_c = 5.6-11$. It should be noted that this value is larger than the expected value of 4.35[34] from the mean field approximation for the *d*-wave superconductors. This gap value will be compared with that in $\kappa$-(BEDT-TTF-d[*n*,*n*])$_2$Cu[N(CN)$_2$]Br in §3.3.

We investigated the temperature dependence of tunneling spectra on $\kappa$-(BEDT-TTF)$_2$Cu(NCS)$_2$.[35] Figure 2 shows tunneling conductance curves obtained on the *b*–*c* plane at several temperatures. The superconducting gap structure is clearly recognized as a dip in the conductance curve for each temperature. The differential conductance at zero bias voltage increases rapidly with increasing temperature. In Fig. 2, the broken line represents the fitting curve using the *d*-wave gap model described as eq. (1), discussed above. In the fitting, the broadening parameter of the one-electron level $\Gamma$ is taken into account as well. The gap structure is well fitted by the calculation with $\Delta_0 = 2.5$ meV for each curve. These temperature dependent curves indicate again that the superconducting gap has the *d*-wave symmetry.

We evaluate the temperature dependence of $\Gamma$, which is obtained from the fitting of the conductance curves shown in Fig. 2. Figure 3 shows the obtained $\Gamma$ as a function of $T/T_c$. It is known that the $\Gamma(T)$ shows the thermally activated dependence at low temperature for the *s*-wave superconductors because of the finite gap on the whole Fermi surface.[33,36] In that case, the activation energy should correspond to the magnitude of the gap. However, in the present case, the exponential curve can hardly fit the observed temperature dependence with the same order of $\Delta_0 = 2.5$ meV obtained from the fitting of the conductance curve. The temperature dependence of $\Gamma$ follows rather the power law than the exponential one. As shown in Fig. 3, the $T^2$-fitting curve $\Gamma(T) = 5.8(T/T_c)^2$, which is represented by the solid line, gives the best fit of the data. The exponent of $\Gamma(T)$ depends on the detailed scattering mechanism of quasi-particles.[36] However, the observed power law dependence is presumably originated from the line nodes of the *d*-wave gap.

As shown in Fig. 2, the conductance at zero bias voltage $dI/dV|_{V=0}$ varies depending on temperature. In order to evaluate the temperature dependence in detail, we plot the zero bias conductance $dI/dV|_{V=0}$ as a function of $T/T_c$ in Fig. 4. Each $dI/dV|_{V=0}(T)$ is normalized to the conductance at the gap edge. The value of $dI/dV|_{V=0}$ increases rapidly

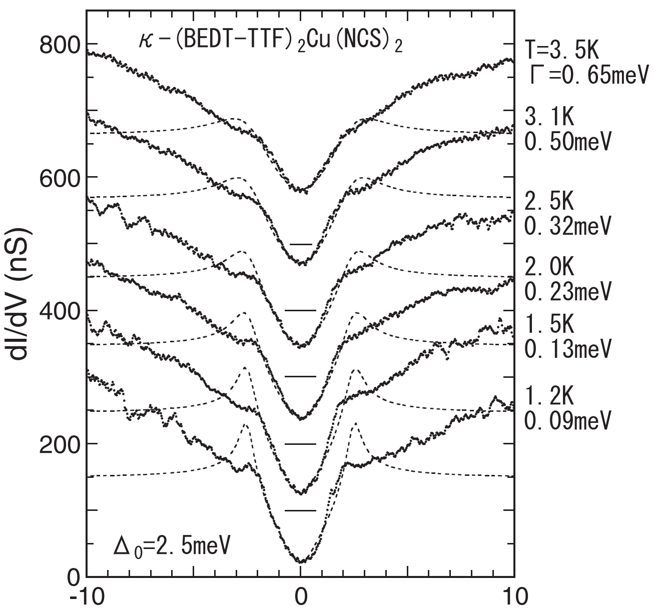


Fig. 2. Tunneling conductance curves obtained on the *b*–*c* plane of $\kappa$-(BEDT-TTF)$_2$Cu(NCS)$_2$ at $T = 1.2$, 1.5, 2.0, 2.5, 3.1, and 3.5 K. The broken line represents the calculated curve using the d-wave gap model with the broadening parameter of the one-electron level $\Gamma$. The zero conductance line of each curve is shifted by 100 nS for clarity.

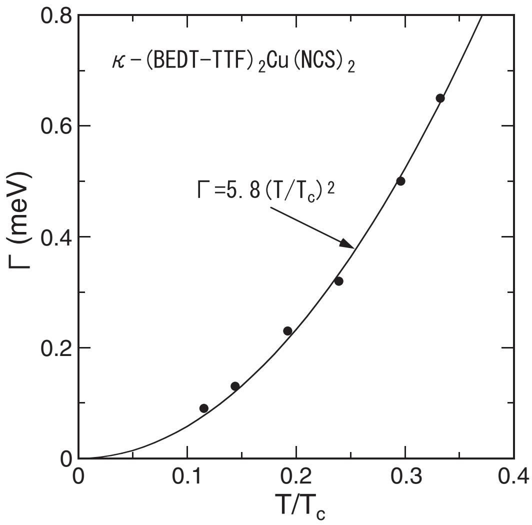


Fig. 3. The broadening parameter $\Gamma$ as a function of $T/T_c$. The solid line represents the fitting curve of $\Gamma(T) = 5.8(T/T_c)^2$.

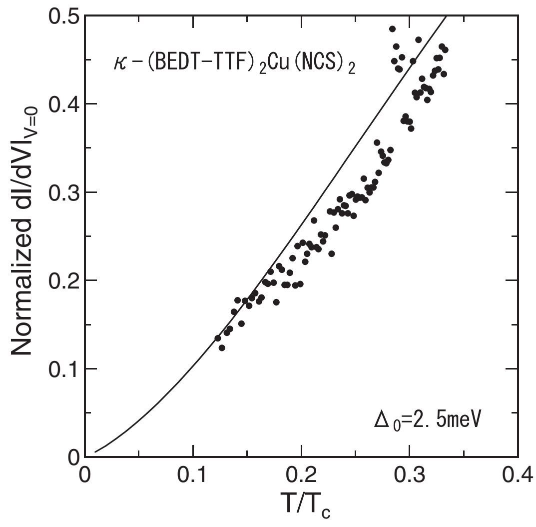


Fig. 4. Temperature dependence of $dI/dV|_{V=0}$. The solid line represents the calculated curve for the *d*-wave gap model with $\Gamma(T) = 5.8(T/T_c)^2$.

with increasing temperature. The dependence is almost linear to the temperature. The solid line in Fig. 4 represents the calculated curve based on the $d$-wave gap model with $\Delta_0 = 2.5$ meV taking the $T^2$-dependence of $\Gamma(T)$ discussed above into account. The zero bias conductance varies much rapidly with the temperature for the $d$-wave gap than the case of the $s$-wave gap. The experimental result of $\mathrm{d}I/\mathrm{d}V|_{V=0}(T)$ is well reproduced by the calculated curve for the $d$-wave gap. The temperature dependence of the zero bias conductance is also consistent with the $d$-wave gap.

It should be emphasized that not only the functional form of the conductance curve at each temperature but also the temperature dependence of tunneling spectra are explained by the $d$-wave pairing symmetry.

### 3.2 Direct observation of the in-plane anisotropy of the order parameter in κ-(BEDT-TTF)$_2$Cu(NCS)$_2$

In order to investigate the in-plane gap anisotropy, we carried out the STS on lateral surfaces of κ-(BEDT-TTF)$_2$-Cu(NCS)$_2$, which are perpendicular to the $b$–$c$ plane.[37] Several conductance curves depending on the surface direction were obtained at lateral surfaces. The results for the surface normal of $\phi = 0$, 70, 30, 56, and 51° are shown in Fig. 5, where $\phi$ denotes the angle from the $c$ axis in the $b$–$c$ plane. The functional form of the conductance curve inside the gap edges varies systematically depending on the surface direction. For $\phi = 0$ and 70°, the curve is flat around $V = 0$ and the gap width is relatively larger. On the other hand, for $\phi = 51$, 56, and 30°, the conductance varies rapidly around $V = 0$ with the bias voltage, and the gap width is relatively smaller. The directional dependence of the conductance curve indicates the fact that the superconducting gap is highly anisotropic in the $b$–$c$ plane.

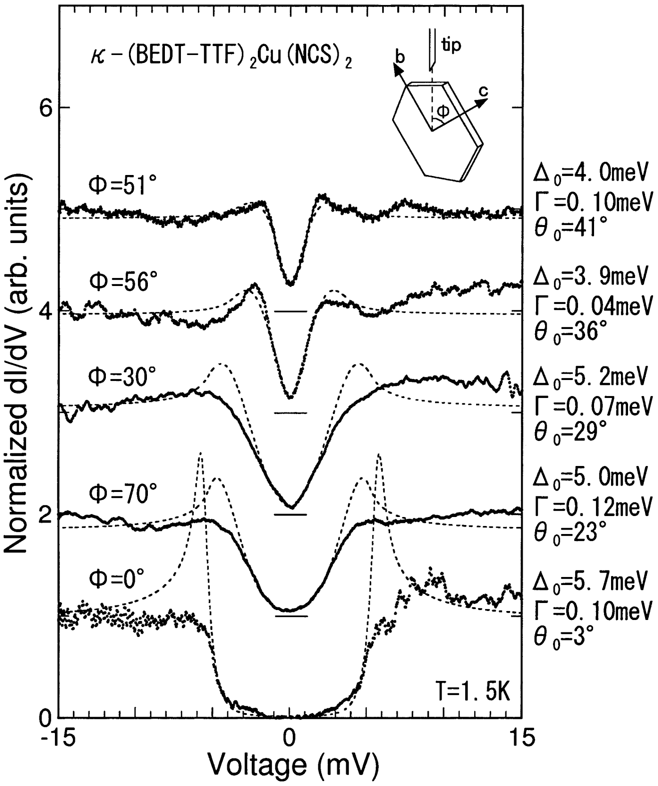


Fig. 5. Tunneling conductance curves on the lateral surfaces of κ-(BEDT-TTF)$_2$Cu(NCS)$_2$ single crystals observed along various tunneling directions at 1.5 K. Curves in the tunneling directions of $\phi = 0°$, 70° ($\phi' = 20°$), 30°, 56° ($\phi' = 34°$), and 51° ($\phi' = 39°$) are shown together, where $\phi$ denotes the angle from the $c$-axis in the $b$–$c$ plane. Each curve is normalized to the conductance at $V = -15$ mV and aligned at intervals of one division for clarity. The broken line represents the calculated curve by the $d$-wave gap model considering the $\boldsymbol{k}$-dependent tunneling.

We try to fit by the model calculation, in which the $\boldsymbol{k}$-dependence of the tunneling transition probability is taken into account. In the calculation, the $d$-wave gap described as $\Delta(\boldsymbol{k}) = \Delta_0 \cos 2\theta$ is assumed again. According to the two-dimensional WKB approximation,[38] the transition probability $p(\theta - \theta_0)$ for the electron with the azimuth $\theta$ of the wave vector $\boldsymbol{k}$ is given as

$$p(\theta - \theta_0) = \exp[-\beta \sin^2(\theta - \theta_0)] \tag{2}$$

with

$$\beta = \frac{E_\mathrm{F}\, d}{\hbar} \sqrt{\frac{2m}{U - E_\mathrm{F}}}. \tag{3}$$

Here $\theta_0$ is the parameter representing the direction perpendicular to the tunneling barrier in $\boldsymbol{k}$ space, $U$ and $d$ are the potential height and width of the tunneling barrier, respectively, and $E_\mathrm{F}$ is the Fermi energy. The dimensionless parameter $\beta$ characterizes the $\boldsymbol{k}$-dependent tunneling. Because of this factor $p$, electrons with large kinetic energy along the barrier normal mainly contribute to the tunneling current. As a result, the conductance curve taking the $\boldsymbol{k}$-dependent tunneling into account is written as

$$\frac{\mathrm{d}I}{\mathrm{d}V} \propto \int_0^{2\pi}\!\!\int_{-\infty}^{\infty} p(\theta - \theta_0)\ \mathrm{Re}\left[\frac{|E - \mathrm{i}\Gamma|}{\sqrt{(E - \mathrm{i}\Gamma)^2 - \Delta^2(\theta)}}\right] \times \left\{-\frac{\partial f(E + eV)}{\partial V}\right\} \mathrm{d}E\, \mathrm{d}\theta. \tag{4}$$

Broken lines in Fig. 5 represent the calculated curves for each direction of $\phi$ with parameters $\Delta_0$, $\Gamma$, and $\theta_0$. In the calculation, the value of $\beta$ is fixed at $\beta = 20$ for the best fitting. This value is relatively larger than the reported value of $\beta = 8$ for $Bi_2Sr_2CaCu_2O_8$[39] probably due to the smaller work function in κ-(BEDT-TTF)$_2$Cu(NCS)$_2$. The systematic change of the functional form of the conductance curve around $V = 0$ is reproduced well. Consequently, the conductance curve observed on the lateral surfaces is also explained by the $d$-wave gap model considering the $\boldsymbol{k}$-dependence of the tunneling transition probability and the fourfold symmetry of the $d$-wave gap discussed below.

The $d$-wave gap has the fourfold symmetry in $\boldsymbol{k}$-space with respect to the magnitude of the gap $|\Delta|$. As a result, we can reduce the azimuthal angle in the $\boldsymbol{k}$-space to the range of $\phi$ to $0 \leq \phi \leq 45°$. Thus, the directions of $\phi = 51$, 56, and 70° are equivalent to $\phi' = 39$, 34, and 20°, respectively, where $\phi'$ denotes the reduced $\phi$. In Fig. 6, the fitting parameter $\theta_0$ is plotted against $\phi'$. The plotted points coarsely show the linear relationship between $\theta_0$ and $\phi'$ which intersects the origin. This means that the direction of line nodes of the gap is $\pi/4$ from the $k_b$ and $k_c$ axes, i.e., the gap has the $d_{x^2-y^2}$-wave symmetry.

As for the node direction, another method has been reported recently. Izawa *et al.*[20] measured the thermal conductivity in the mixed state of κ-(BEDT-TTF)$_2$Cu(NCS)$_2$

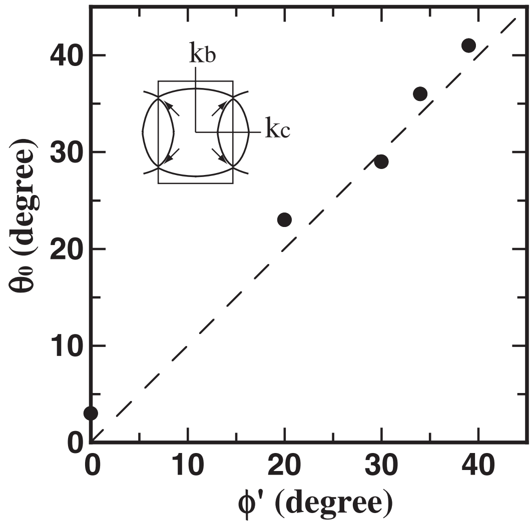


Fig. 6. Fitting parameter $\theta_0$ against $\phi'$. Inset: The Fermi surface of $\kappa$-(BEDT-TTF)$_2$Cu(NCS)$_2$. Arrows represent node directions determined by the STS at lateral surfaces.

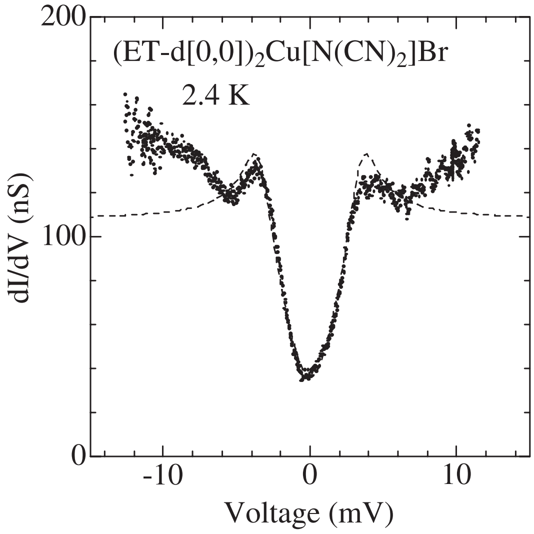


Fig. 7. Typical tunneling conductance curve obtained at the $a$–$c$ $\kappa$-(BEDT-TTF-d[0,0])$_2$Cu[N(CN)$_2$]Br at 2.4 K. The broken line represents the calculated curve for the $d$-wave gap model with $\Delta_0 = 3.5$ meV and $\Gamma = 0.53$ meV.

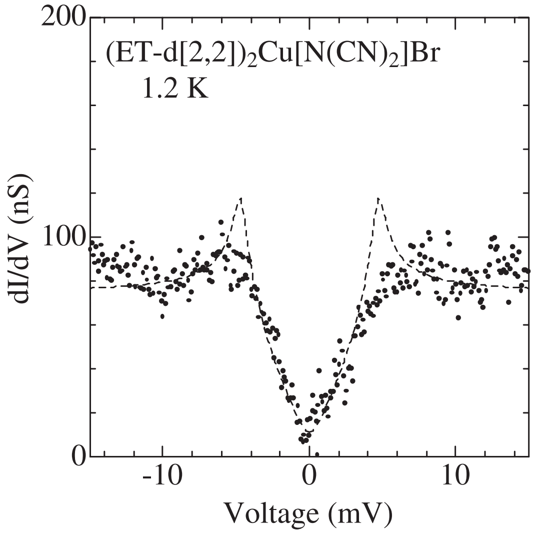


Fig. 8. Typical tunneling conductance curve obtained at the $a$–$c$ $\kappa$-(BEDT-TTF-d[2,2])$_2$Cu[N(CN)$_2$]Br at 1.2 K. The broken line represents the calculated curve for the $d$-wave gap model with $\Delta_0 = 4.7$ meV and $\Gamma = 0.24$ meV.

by rotating the magnetic field in the conducting plane and discussed the gap anisotropy in terms of the Doppler shift of the quasi-particle energy spectrum. The angular dependence of the electronic thermal conductivity $\kappa^{el}(\theta)$, where $\theta$ is the field direction from the $b$ axis, has a fourfold symmetry with minima at $\pi/4$ from the $b$ and $c$ axes. In the case of the $d$-wave, $\kappa^{el}(\theta)$ is calculated to have minima when the magnetic field is parallel to the node direction.[41] They concluded that the gap has nodes along $\pi/4$ from $k_b$ and $k_c$ axes. Accordingly, the node direction determined in our STS on the lateral surfaces is consistent with their results.

As the origin of the attractive interaction, the $d_{xy}$-wave symmetry is naively expected from the spin fluctuation.[4–6] On the other hand, the fluctuation exchange (FLEX) approximation[40] suggests the competition between the $d_{x^2-y^2}$ and $d_{xy}$-wave symmetry with respect to the dimerization strength. Our conclusion from the STS is the $d_{x^2-y^2}$-wave symmetry in $\kappa$-(BEDT-TTF)$_2$Cu(NCS)$_2$ and is inconsistent with the former at least.

We could not observe the ZBCP, which is associated to the line node in the $d$-wave superconductors, in the measurement on lateral surfaces of $\kappa$-(BEDT-TTF)$_2$-Cu(NCS)$_2$. Some reasons why we can not observe the ZBCP will be discussed in §3.5.

### 3.3 *Tunneling spectra of partially deuterated $\kappa$-(BEDT-TTF)$_2$Cu[N(CN)$_2$]Br*

The superconducting phase of protonated and partially deuterated $\kappa$-(BEDT-TTF-d[$n$,$n$])$_2$Cu[N(CN)$_2$]Br was also studied. In the following, we call $\kappa$-(BEDT-TTF-d[$n$,$n$])$_2$-Cu[N(CN)$_2$]Br as d[$n$,$n$] salt. Tunneling spectra were obtained at the conducting $a$–$c$ plane, in d[0,0],[42] d[2,2][43] and d[3,3][44] salts. Figures 7–9 show typical tunneling conductance curves for d[0,0], d[2,2] and d[3,3] salts, respectively. The superconducting gap is clearly observed in all salts. Broken lines in Figs. 7–9 represent the $d$-wave calculation curves using eq. (1). Parameters used in the fitting are $\Delta_0 = 3.5$ meV and $\Gamma = 0.53$ meV for d[0,0], $\Delta_0 = 4.7$ meV and $\Gamma = 0.24$ meV for d[2,2] and $\Delta_0 = 1.8$ meV and $\Gamma = 0.36$ meV for d[3,3]. Tunneling spectra are explained by the the $d$-wave gap model similarly to the tunneling at the conducting plane of $\kappa$-(BEDT-TTF)$_2$-Cu(NCS)$_2$ as mentioned in §3.1. It is noted that the conductance at zero bias voltage for $\kappa$-(BEDT-TTF-d[$n$,$n$])$_2$-Cu[N(CN)$_2$]Br is larger than that in $\kappa$-(BEDT-TTF)$_2$-Cu(NCS)$_2$. The value of $\Gamma$ is a few times larger than that in $\kappa$-(BEDT-TTF)$_2$Cu(NCS)$_2$. We think that larger $\Gamma$ is due to some disorder which is presumably related to 80 K anomaly[45] in $\kappa$-(BEDT-TTF-d[$n$,$n$])$_2$Cu[N(CN)$_2$]Br. However, the obtained $\Gamma$ is still much smaller than the gap value $\Delta_0$. It assures again the validity of the discussion about the pairing symmetry.

Gap parameters for these salts are listed in Table I together with that for $\kappa$-(BEDT-TTF)$_2$Cu(NCS)$_2$. The scatter

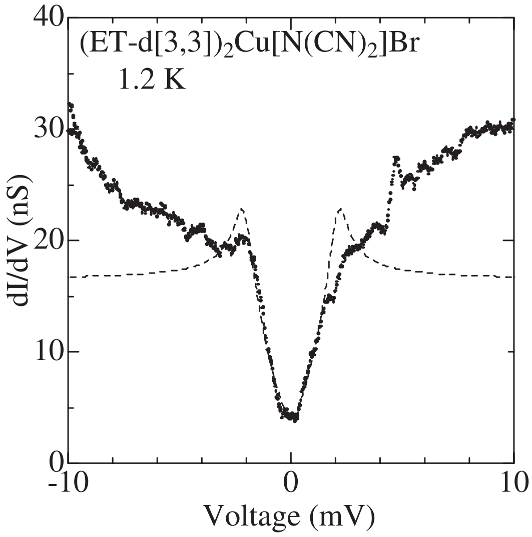


Fig. 9. Typical tunneling conductance curve obtained at the *a–c* $\kappa$-(BEDT-TTF-d[3,3])$_2$Cu[N(CN)$_2$]Br at 1.2 K. The broken line represents the calculated curve for the *d*-wave gap model with $\Delta_0 = 1.8$ meV and $\Gamma = 0.36$ meV.

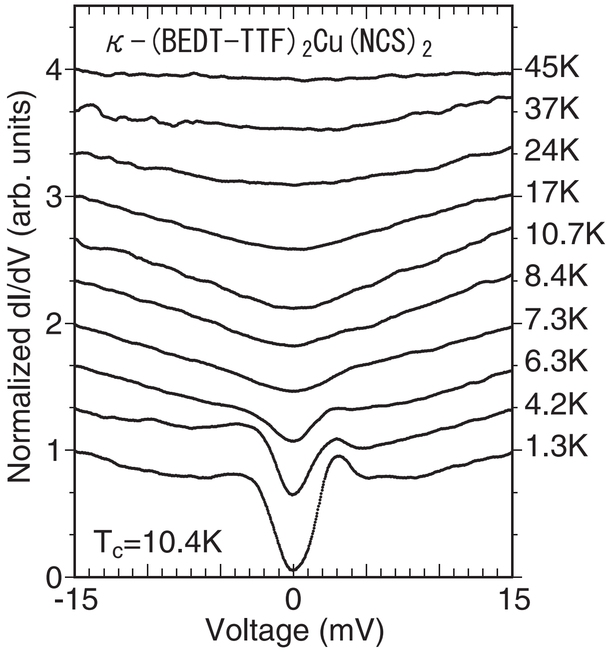


Fig. 10. Temperature dependence of tunneling spectra on the *b–c* plane of $\kappa$-(BEDT-TTF)$_2$Cu(NCS)$_2$.

Table I. Gap parameter $\Delta_0$ and corresponding $2\Delta_0/kT_c$ for $\kappa$-(BEDT-TTF)$_2$Cu(NCS)$_2$, which is denoted as NCS, and $\kappa$-(BEDT-TTF-d[*n*,*n*])$_2$Cu[N(CN)$_2$]Br, which is denoted as d[*n*,*n*].

| | $\Delta_0$ (meV) | $2\Delta_0/kT_c$ |
|---|---|---|
| NCS | 2.5–4.9 | 5.6–11 |
| d[2,2] | 3.0–4.8 | 5.8–9.3 |
| d[3,3] | 1.4–3.3 | 2.7–6.4 |
| d[0,0] | 2.1–3.9 | 4.3–7.9 |

in value of $\Delta_0$ is due to the sample dependence. The ratio of the on-site Coulomb interaction $U$ to the band width $W$ becomes larger by the deuteration of end protons in BEDT-TTF molecule and the system approaches to the Mott boundary. In comparison between d[0,0] and d[2,2], it is deduced that the reduced gap parameter $2\Delta_0/kT_c$ increases with increasing $U/W$. However, the reduced gap for d[3,3] salt is smaller than those for both d[0,0] and d[2,2] salt. We find that $2\Delta_0/kT_c$ does not increase monotonically toward the Mott boundary. In addition, the value for $\kappa$-(BEDT-TTF)$_2$Cu(NCS)$_2$, which has smaller $U/W$ than d[0,0] salts, is almost the same as that for d[2,2] salt. The dependence is rather complicated. It is our future work to study the slowly cooled d[4,4] salt, which is located just on the boundary between superconducting and antiferromagnetic insulating phase.

It is noteworthy that the value of $2\Delta_0/kT_c$ for $\kappa$-(BEDT-TTF-d[*n*,*n*])$_2$Cu[N(CN)$_2$]Br and $\kappa$-(BEDT-TTF)$_2$Cu(NCS)$_2$ is larger than the prediction of 4.35 from the mean field theory for the *d*-wave superconductors.[34] It suggests the strong coupling superconductivity in $\kappa$-(BEDT-TTF)$_2$X$_2$. Similar value of $2\Delta_0/kT_c$ was reported in high-$T_c$ cuprates.[46] Large value of $2\Delta_0/kT_c$ was also reported in layered nitride superconductor ZrNCl$_{0.7}$.[47]

### 3.4 *Pseudogap above $T_c$*

Here we discuss the temperature dependence of tunneling spectra at higher temperature region. Figure 10 shows the temperature dependence of tunneling conductance curves obtained on the *b–c* plane of $\kappa$-(BEDT-TTF)$_2$Cu(NCS)$_2$. Each conductance curve is normalized to the conductance at $V = -15$ mV. At $T = 1.3$ K, the superconducting gap is clearly recognized. With increasing temperature, the conductance around the zero bias voltage increases rapidly and the gap structure becomes smeared. Peaks at the gap edge disappear at about 8.4 K. There is no noticeable change across $T_c$ of 10.4 K. The broad dip structure still remains even above $T_c$. The depth of the dip decreases with increasing temperature. The conductance curve becomes flat above 45 K. The temperature dependence differs remarkably from conventional superconductors, in which the tunneling spectra become flat just above $T_c$. The broad dip above $T_c$ could be assigned as the pseudogap.

The pseudogap above $T_c$ has been reported in high-$T_c$ cuprates.[48,49] However, there is the significant difference in tunneling spectra between $\kappa$-(BEDT-TTF)$_2$Cu(NCS)$_2$ and high-$T_c$ oxides. The magnitude of the pseudogap is larger than 15 meV in $\kappa$-(BEDT-TTF)$_2$Cu(NCS)$_2$ while the superconducting gap is $\Delta_0 \sim 3$ meV. In high-$T_c$ cuprates, on the other hand, the gap structure with the same magnitude as the superconducting gap persists above $T_c$ as the pseudogap. The superconducting gap is connected to the pseudogap continuously. The conductance peaks at the gap edge still exist just above $T_c$ in high-$T_c$ cuprates. Accordingly, the origin of the pseudogap might be different between $\kappa$-(BEDT-TTF)$_2$Cu(NCS)$_2$ and high-$T_c$ cuprates. However, it should be noted that the pseudogap is the common feature in the superconductivity with the highly correlated electron system.

Figures 11 and 12 show tunneling conductance curves at various temperature obtained on the *a–c* plane of d[0,0] and

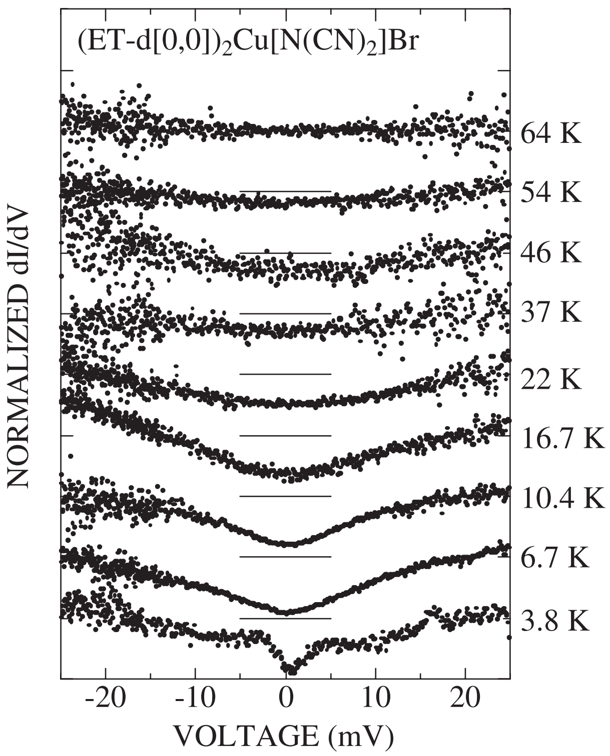


Fig. 11. Temperature dependence of tunneling spectra on the *a*–*c* plane of $\kappa$-(BEDT-TTF-d[0,0])$_2$Cu[N(CN)$_2$]Br. The horizontal bar represents the zero conductance line for each curve.

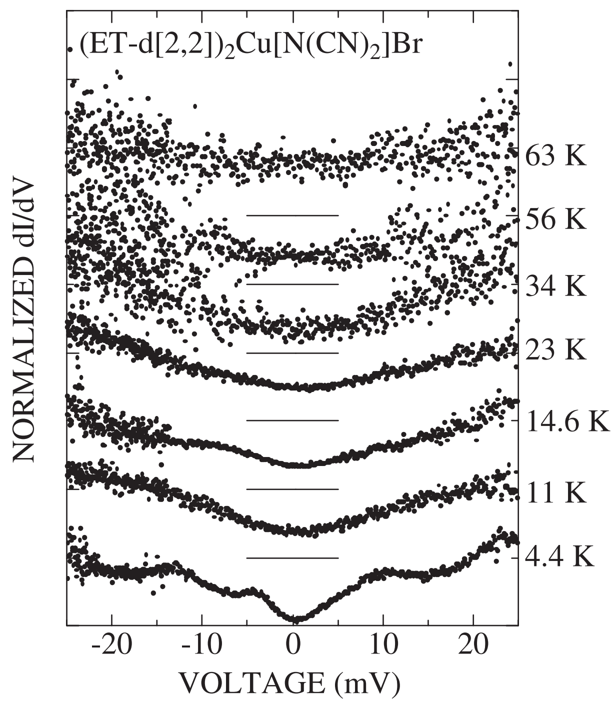


Fig. 12. Temperature dependence of tunneling spectra on the *b*–*c* plane of $\kappa$-(BEDT-TTF-d[0,0])$_2$Cu[N(CN)$_2$]Br. The horizontal bar represents the zero conductance line for each curve.

d[2,2] salts, respectively. Essentially the same behavior is observed as in $\kappa$-(BEDT-TTF)$_2$Cu(NCS)$_2$. The broad dip structure is found above $T_c$ in each salt. The pseudogap has the magnitude of larger than 20 meV. In $\kappa$-(BEDT-TTF)$_2$-Cu(NCS)$_2$, the pseudogap disappears at 45 K as described above. The temperature, at which the pseudogap disappears, is estimated as about 55 K both in d[0,0] and d[2,2] salts. It is noteworthy that these temperatures are almost the same as the temperature, in which the magnetic anomalies are observed. The enhancement of nuclear spin–lattice relaxation rate $(T_1T)^{-1}$ and the rapid decrease in the Knight shift were observed at 50 K in $^{13}$C NMR.[50,51] The static magnetic susceptibility also decreases rapidly below 50 K.[52] These facts imply that the origin of the pseudogap is related to the spin fluctuation.

We also note that the pseudogap is found in $\kappa$-(MDT-TTF)$_2$AuI$_2$[53] ($T_c = 4$ K), which is the organic superconductor with asymmetric donor molecules. The *d*-wave is also suggested for its gap symmetry by the STS.

### *3.5 Zero bias conductance peak*

It should be noted that the anomalous enhancement of conductance around $V = 0$ is observed sometimes in $\kappa$-(BEDT-TTF-d[3,3])$_2$Cu[N(CN)$_2$]Br. Figure 13 shows the tunneling spectra with such anomaly. Curves for two different samples are shown together. The tunneling conductance at $V = 0$ increases divergently in contrast to the case of the superconducting gap. We think that this sharp peak corresponds to the ZBCP which is associated with the line node in the *d*-wave superconductors.

The ZBCP has been found in high-$T_c$ cuprates Bi$_2$Sr$_2$-CaCu$_2$O$_8$,[29] La$_{2-x}$Sr$_x$CuO$_4$[30] and YBa$_2$Cu$_3$O$_7$.[31] The present result is the first observation of the ZBCP in the organic superconductor $\kappa$-(BEDT-TTF)$_2$X. The ZBCP is caused by the zero energy state, which is the bound state formed around gap nodes where the sign of the order parameter changes.[28] The essential point of the origin of the bound state is that electron and hole like quasi-particles, which

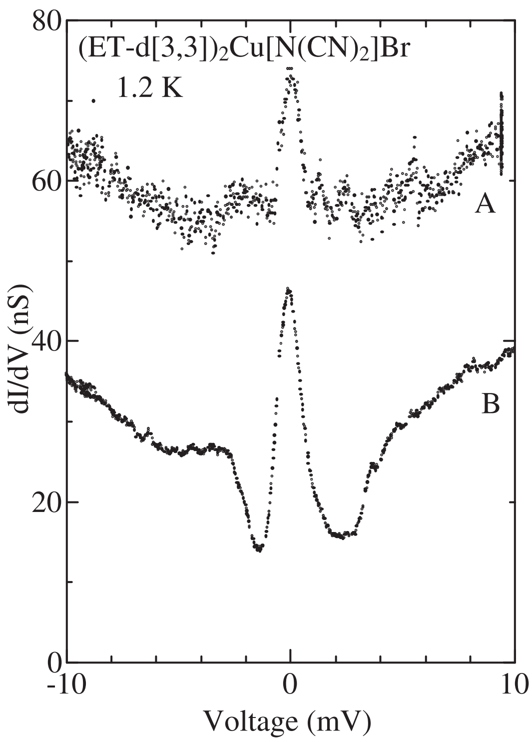


Fig. 13. Tunneling spectra with the zero bias anomaly. Curves for two different samples are shown together. The zero conductance line of each curve is shifted by 20 nS for clarity.

come from injected electrons into superconductor, feel opposite sign of pair potentials. It should be noted that the ZBCP is the phase sensitive phenomenon. Therefore, the ZBCP is a direct evidence for nodes of the superconducting gap.

Normally, one can hardly observe the ZBCP in the present tunneling configuration, in which electrons tunnel perpendicular to the conducting plane. As a result, the in-plane anisotropy would be averaged out. It is essential in observation of the ZBCP that electrons with wave number around the gap nodes contribute selectively to the tunneling. We deduce that micro steps or some disorder of the surface enabled us to observe the ZBCP. The in-plane component of the wave number can be selected in the tunneling from step edges. Actually, the ZBCP was sometimes observed at the $c$-direction tunneling in high-$T_c$ cuprates. In addition, domain boundaries between the superconducting and insulating phases might help the tunneling electron to flow along the conducting plane in $\kappa$-(BEDT-TTF-d[3,3])$_2$Cu[N(CN)$_2$]Br.

We could not find the ZBCP in the tunneling at lateral surfaces for $\kappa$-(BEDT-TTF)$_2$Cu(NCS)$_2$ in contrast to the present results on $\kappa$-(BEDT-TTF-d[3,3])$_2$Cu[N(CN)$_2$]Br. One possible reason is that we could not probe the tunneling along the just node direction in the previous work on lateral surfaces. The ZBCP is sensitive to the direction of the wave vector of tunneling electrons. The directional dependent tunneling is discussed according to WKB approximation as in §3.2. The tilting angle of the wave vector $\boldsymbol{k}$ from the surface normal, in which the tunneling probability decays by a factor of $e$, in our STS configuration on BEDT-TTF salts is estimated as 13° from eq. (2) with $\beta = 20$. The angle window is narrower than that for $Bi_2Sr_2CaCu_2O_8$ of 22°. A small tilting from the node direction makes difficult to observe the ZBCP.

Another possible reason is difference in the geometry of the Fermi surface. For $\kappa$-(BEDT-TTF)$_2$Cu(NCS)$_2$, the Fermi surface is separated at the zone boundary due to the asymmetrical arrangement of anions.[54] As a result, the gap opens at the direction around $\pi/4$ from $k_b$- and $k_c$-axes. It suggests that there is no metallic state around gap nodes. Therefore, it is possible that no ZBCP is intrinsically observed for $\kappa$-(BEDT-TTF)$_2$Cu(NCS)$_2$. On the other hand, there is no such gap on the Fermi surface for $\kappa$-(BEDT-TTF)$_2$Cu[N(CN)$_2$]Br because of the symmetric anion arrangement.[55] From this point of view, $\kappa$-(BEDT-TTF)$_2$-Cu[N(CN)$_2$]Br is suitable to study the ZBCP.

In bulk single crystals of $\kappa$-(BEDT-TTF)$_2$Cu[N(CN)$_2$]Br, the (100) surface can be obtained easily. This fact implies that the (100) surface is exposed frequently as micro step edges. The configuration, where the ZBCP is observed, might attribute to the (100) micro step edge in $\kappa$-(BEDT-TTF-d[3,3])$_2$Cu[N(CN)$_2$]Br. It corresponds to the $d_{xy}$-wave symmetry. The above speculation suggests the possibility of difference of the node direction between these salts; the $d_{x^2-y^2}$-wave for $\kappa$-(BEDT-TTF)$_2$Cu(NCS)$_2$ and the $d_{xy}$-wave symmetry for $\kappa$-(BEDT-TTF-d[3,3])$_2$Cu[N(CN)$_2$]Br may be realized. Kuroki *et al.*[40] reported that $d_{x^2-y^2}$ and $d_{xy}$-wave symmetries compete depending on the dimerization strength. Accordingly, the determination of the node direction in $\kappa$-(BEDT-TTF)$_2$Cu[N(CN)$_2$]Br might be an essential key for the origin of the attractive interaction. The STS at lateral surfaces in $\kappa$-(BEDT-TTF)$_2$Cu[N(CN)$_2$]Br is our future problem to determine the direction of nodes.

## 4. Conclusions

The superconducting gap structure in organic superconductors $\kappa$-(BEDT-TTF)$_2$X was investigated by the tunneling measurement with use of the STS. Tunneling spectra were obtained both on the conducting $b$–$c$ plane and lateral surfaces of single crystals of $\kappa$-(BEDT-TTF)$_2$-Cu(NCS)$_2$. The observed tunneling conductance curve is well explained by the $d$-wave gap symmetry. The temperature dependence of tunneling spectra far below $T_c$ is also consistent with the $d$-wave symmetry taking into account the $T^2$-dependence of the one-electron level broadening. In-plane gap anisotropy was clearly observed in tunneling spectra on lateral surfaces varying the tunneling direction. The directional dependence is also explained by the $d$-wave symmetry with the $\boldsymbol{k}$-dependence of the tunneling transition probability based on the WKB approximation. The node direction is determined as $\pi/4$ from the $k_b$- and $k_c$-axes. It indicates that the superconducting pair wave function in $\kappa$-(BEDT-TTF)$_2$Cu(NCS)$_2$ has the $d_{x^2-y^2}$-wave symmetry. Protonated and partially deuterated $\kappa$-(BEDT-TTF)$_2$-Cu[N(CN)$_2$]Br were also studied and understood as the $d$-wave gap symmetry as well. Large value of $2\Delta/kT_c$ in all salts suggests the strong coupling superconductivity. The pseudogap structure is observed above $T_c$ both in $\kappa$-(BEDT-TTF)$_2$Cu(NCS)$_2$ and $\kappa$-(BEDT-TTF-d[$n$,$n$])$_2$Cu[N(CN)$_2$]Br. We also observed the ZBCP in $\kappa$-(BEDT-TTF-d[3,3])$_2$-Cu[N(CN)$_2$]Br, as an evidence of nodes of the superconducting gap for the first time in the organic superconductor.

**Acknowledgements**

We would like thank Professor H. Anzai and Professor J. Yamada for useful advices on the crystal growth. We also would like to thank Professor A. Kawamoto for providing single crystals of $\kappa$-(BEDT-TTF-d[$n$,$n$])$_2$Cu[N(CN)$_2$]Br. This work was supported in part by a Grant-in-Aid for Scientific Research (No. 16038203) from the Ministry of Education, Culture, Sports, Science and Technology.

1) T. Ishiguro, K. Yamaji and G. Saito: *Organic Superconductors* (Springer, Berlin, 1998) 2nd ed.
2) K. Kanoda: Hyperfine Interactions **104** (1997) 235.
3) B. Batllog and V. J. Emery: Nature **382** (1996) 20.
4) R. Arita, K. Kuroki and H. Aoki: J. Phys. Soc. Jpn. **69** (2000) 1181.
5) B. J. Powell and R. H. McKenzie: Phys. Rev. B **69** (2004) 024519.
6) J. X. Li: Phys. Rev. Lett. **91** (2003) 037002.
7) S. M. De Soto, C. P. Slichter, A. M. Kini, H. H. Wang, U. Geiser and J. M. Williams: Phys. Rev. B **52** (1995) 10364.
8) H. Mayaffre, P. Wzietek, D. Jérome, C. Lenoir and P. Batail: Phys. Rev. Lett. **75** (1995) 4122.
9) K. Kanoda, K. Miyagawa, A. Kawamoto and Y. Nakazawa: Phys. Rev. B **54** (1996) 76.
10) Y. Nakazawa and K. Kanoda: Phys. Rev. B **55** (1997) R8670.
11) K. Kanoda, K. Akiba, K. Suzuki, T. Takahashi and G. Saito: Phys. Rev. Lett. **65** (1990) 1271.
12) L. P. Le, G. M. Luke, B. J. Sternlieb, W. D. Wu, Y. J. Uemura, J. H. Brewer, T. M. Riseman, C. E. Stronach, G. Saito, H. Yamochi, H. H. Wang, A. M. Kini, K. D. Carlson and J. M. Williams: Phys. Rev. Lett. **68** (1992) 1923.
13) D. Achkir, M. Poirier, C. Bournonnais, G. Quirion, C. Lenoir, P. Batail and D. Jérome: Phys. Rev. B **47** (1993) 11595.

14) A. Carrington, I. J. Bonalde, R. Prozorov, R. W. Giannetta, A. M. Kini, J. Schlueter, H. H. Wang, U. Geiser and J. M. Williams: Phys. Rev. Lett. **83** (1999) 4172.
15) M. Pinterić, S. Tomić, M. Prester, D. Drobac, O. Milat, K. Maki, D. Schweitzer, I. Heinen and W. Strunz: Phys. Rev. B **61** (2000) 7033.
16) M. Lang, N. Toyota, T. Sasaki and H. Sato: Phys. Rev. Lett. **69** (1992) 1443.
17) M. Dressel, S. Bruder, G. Gruner, K. D. Carlson, H. H. Wang and J. M. Williams: Phys. Rev. B **48** (1993) 9906.
18) D. R. Harshman, A. T. Fiory, R. C. Haddon, M. L. Kaplan, T. Pfiz, E. Koster, I. Shinkoda and D. Ll. Williams: Phys. Rev. B **49** (1994) 12990.
19) H. Elsinger, J. Wosnitza, S. Wanka, J. Hagel, D. Schweitzer and W. Strunz: Phys. Rev. Lett. **84** (2000) 6098.
20) K. Izawa, H. Yamaguchi, T. Sasaki and Y. Matsuda: Phys. Rev. Lett. **88** (2002) 027002.
21) I. Gieaver: Phys. Rev. Lett. **5** (1960) 147.
22) H. F. Hess, R. B. Robinson, R. C. Dynes, J. M. Valles, Jr. and J. V. Waszczak: Phys. Rev. Lett. **62** (1989) 214.
23) S. H. Pan, E. W. Hudson, K. M. Lang, H. Eisaki, S. Uchida and J. C. Davis: Nature **403** (2000) 746.
24) K. Nomura, K. Nagao, K. Ichimura and N. Matsunaga: Synth. Met. **70** (1995) 911.
25) K. Ichimura, T. Arai, K. Nomura, S. Takasaki, J. Yamada, S. Nakatsuji and H. Anzai: Synth. Met. **103** (1999) 1812.
26) H. Bando, S. Kashiwaya, H. Tokumoto, H. Anzai, N. Kinoshita and K. Kajimura: J. Vac. Sci. Technol. A **8** (1990) 479.
27) A. Kawamoto, H. Taniguchi and K. Kanoda: J. Am. Chem. Soc. **120** (1998) 10984.
28) S. Kashiwaya and Y. Tanaka: Rep. Prog. Phys. **63** (2000) 1641.
29) K. Suzuki, K. Ichimura, K. Nomura and S. Takekawa: J. Phys.: Condens. Matter **11** (1999) 3133.
30) S. Tanaka, E. Ueda, M. Sato, K. Tamasaku and S. Uchida: J. Phys. Soc. Jpn. **64** (1995) 1476.
31) S. Kashiwaya, Y. Tanaka, H. Takashima, Y. Koyanagi and K. Kajimura: Phys. Rev. B **51** (1995) 1350.
32) H. Anzai, J. M. Delrieu, S. Takasaki, S. Nakatsuji and J. Yamada: J. Cryst. Growth **154** (1995) 145.
33) R. C. Dynes, V. Narayanamurti and J. P. Garno: Phys. Rev. Lett. **41** (1978) 1509.
34) F. J. Ohkawa: J. Phys. Soc. Jpn. **56** (1987) 2267.
35) T. Arai, K. Ichimura, K. Nomura, S. Takasaki, J. Yamada, S. Nakatsuji and H. Anzai: Solid State Commun. **116** (2000) 679.
36) S. B. Kaplan, C. C. Chi, D. N. Langenberg, J. J. Chang, S. Jafarey and D. J. Scalapino: Phys. Rev. B **14** (1976) 4854.
37) T. Arai, K. Ichimura, K. Nomura, S. Takasaki, J. Yamada, S. Nakatsuji and H. Anzai: Phys. Rev. B **63** (2001) 104518.
38) E. L. Wolf: *Principles of Electron Tunneling Spectroscopy* (Oxford University Press, New York, 1989) p. 21.
39) K. Suzuki, K. Ichimura, K. Nomura and S. Takekawa: Phys. Rev. Lett. **83** (1999) 616.
40) K. Kuroki, K. Kimura, R. Arita, Y. Tanaka and Y. Matsuda: Phys. Rev. B **65** (2002) 100516.
41) I. Vekhter, P. J. Hirschfeld, J. P. Carbotte and E. J. Nicol: Phys. Rev. B **59** (1999) R9023.
42) K. Ichimura, K. Suzuki, K. Nomura and A. Kawamoto: Synth. Met. **133–134** (2003) 213.
43) K. Ichimura, K. Suzuki, K. Nomura and A. Kawamoto: Synth. Met. **137** (2003) 1229.
44) K. Ichimura, S. Higashi, K. Nomura and A. Kawamoto: Synth. Met. **153** (2005) 409.
45) X. Su, F. Zuo, J. A. Schlueter, A. M. Kini and J. M. Williams: Phys. Rev. B **58** (1998) R2944.
46) K. Ichimura, K. Suzuki, K. Nomura and S. Takekawa: J. Phys.: Condens. Matter **7** (1995) L545.
47) T. Takasaki, T. Ekino, H. Fujii and S. Yamanaka: J. Phys. Soc. Jpn. **74** (2005) 2586.
48) Ch. Renner, B. Ravaz, J. Y. Genoud, K. Kadowaki and Ø. Fischer: Phys. Rev. Lett. **80** (1998) 149.
49) M. Suzuki, T. Watanabe and A. Matsuda: Phys. Rev. Lett. **82** (1999) 5361.
50) H. Mayaffre, P. Wzietek, D. Jérome, C. Lenoir and P. Batail: Europhys. Lett. **28** (1994) 205.
51) A. Kawamoto, K. Miyagawa, Y. Nakazawa and K. Kanoda: Phys. Rev. Lett. **74** (1995) 3455.
52) T. Sasaki, N. Yoneyama, A. Matsuyama and N. Kobayashi: Phys. Rev. B **65** (2002) 060505.
53) K. Ichimura, K. Nomura, T. Nakamura, T. Takahashi, B. Hilti and J. S. Zambounis: Synth. Met. **103** (1999) 1873.
54) K. Oshima, T. Mori, H. Inokuchi, H. Urayama, H. Yamochi and G. Saito: Phys. Rev. B **38** (1988) 938.
55) U. Geiser, A. J. Schultz, H. H. Wang, D. M. Watkins, D. L. Stupka, J. M. Williams, J. E. Shirber, D. L. Overmyer, D. Jung, J. J. Nova and M. H. Whangbo: Physica C **174** (1991) 475.

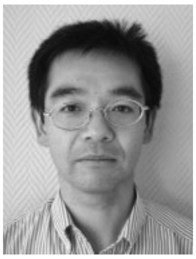

**Koichi Ichimura** was born in Tochigi Prefecture, Japan in 1965. He obtained his B. Sc (1988), M. Sc. (1990) and Ph. D. (1993) degrees from Hokkaido University. Since 1994 he has been a research associate at Graduate School of Science, Hokkaido University. He has studied the electronic state in low-dimensional conductors by low temperature STM/STS. The charge density wave and superconductivity in nano-topological crystals have also been of interest to him.

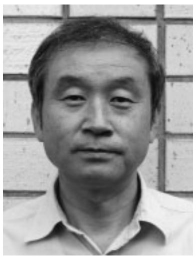

**Kazushige Nomura** was born in Ishikawa Prefecture, Japan in 1951. He obtained his B. Sc. (1974), M. Sc. (1976) and D. Sc. (1979) degrees from the University of Tokyo. He was a research associate (1979–1985) at Faculty of Science, Tokyo Metropolitan University. Then he moved as a lecturer (1985–1987) at Faculty of Science, Hokkaido University. After an associate professor (1987–1994) and a professor (1994–1995) at Faculty of Science, he has been a professor at Graduate School of Science, Hokkaido University since 1995. He has worked on the low-dimensional electron systems by means of STM, NMR and electric transports.